Appl. Phys. B 72, 793–801 (2001) / Digital Object Identifier (DOI) 10.1007/s003400100559

Applied Physics B
Lasers
and Optics

Low-threshold mid-infrared optical parametric oscillation in periodically poled $LiNbO_3$ synchronously pumped by a Ti:sapphire laser

M. Ebrahimzadeh*, P.J. Phillips, S. Das**

School of Physics and Astronomy, University of St Andrews, North Haugh, St Andrews, Fife KY16 9SS, Scotland, UK

Received: 5 December 2000/Revised version: 23 January 2001/Published online: 27 April 2001 –

Abstract. We report the generation of tunable high-repetition-rate optical pulses in the mid-infrared using synchronously pumped parametric oscillation in periodically poled $LiNbO_3$ (PPLN). Using a Kerr-lens-mode-locked Ti:sapphire laser as the pump source and a PPLN crystal incorporating grating periods of 21.0–22.4 μm, we have achieved wavelength conversion in the 4–6-μm spectral range in the mid-infrared. The use of a semi-monolithic cavity design and hemispherical focusing has permitted pulse generation in the strong idler absorption region of PPLN, resulting in a simple, compact, all-solid-state configuration with a pump power threshold as low as 17 mW and mid-infrared idler powers of up to 64 mW at 9% extraction efficiency. Signal output powers of up to 280 mW at 35% extraction efficiency are available over the 1.004–1.140-μm spectral range at 80.5 MHz and pulse repetition rates at harmonics of the fundamental frequency up to 322 MHz have also been obtained.

PACS: 42.55; 42.60; 42.65

The generation of tunable high-repetition-rate pulses with picosecond and femtosecond durations in the mid-infrared is attractive for a variety of applications including time-resolved spectroscopy of semi-conductors. The 4–6-μm spectral range is of particular interest for the study of inter-subband transitions, scattering mechanisms, or Auger recombination and suppression in narrow-band-gap semi-conductors such as InSb, InAlAs and InAsSb. Due to the absence of conventional laser sources in this spectral range, optical parametric oscillators (OPOs) synchronously pumped by mode-locked lasers offer promising alternatives for the generation of such radiation. They can provide continuous tunability over extended wavelength regions, practical output power and sufficiently narrow bandwidth to meet the requirements of many applications.

*Corresponding author.
(Fax: +44-1334/463-104, E-mail: me@st-andrews.ac.uk)
**_Permanent address_: Department of Physics, The University of Burdwan, Golapbag, Burdwan 713 104, India

Due to a broad infrared transmission range and large figure-of-merit, classical nonlinear crystals such as $AgGaS_2$, $AgGaSe_2$, $ZnGeP_2$, $CdGeAs_2$ could be promising material candidates for near and mid-infrared OPOs. However, because of comparatively large absorption near the band-edge in these crystals (except in $AgGaS_2$), the required pump sources need to be at wavelengths $> 1\,\mu m$. At the same time, a general lack of noncritical phase matching (NCPM) in these materials for mid-infrared parametric generation often necessitates the use of high-power laser sources to overcome the detrimental effects of spatial walk-off. The deficiency of NCPM in these materials can be overcome by using mixed chalcopyrite crystals such as $AgGa_xIn_{1-x}Se_2$ [1–4], $AgGa(S_xSe_{1-x})_2$ [5], $CdGe(P_xAs_{1-x})_2$ [6], $AgGa_xIn_{1-x}S_2$ [7], where birefringence can be adjusted by judicial mixing of the parent crystals. However, these crystals are still in the development stage, although recently a temperature-tuned NCPM OPO pumped at 2.13 μm in $AgGa_xIn_{1-x}Se_2$, having an In concentration of 28.8%, has been reported [2]. Combined with the restricted availability of practical picosecond laser sources in the near-infrared these factors have confined the choice of the pump source predominantly to high-power mode-locked Nd-based lasers, limiting the widespread development of high-repetition-rate near and mid-infrared OPOs based on classical materials.

Presently, with the advent of periodically poled nonlinear crystals, there has been renewed interest in the development of high-repetition-rate synchronously pumped OPOs tunable in the near and mid-infrared using low- to moderate-power pump sources. A quasi-phase-matched (QPM) material has several advantages over birefringent phase matching [8]. It provides access to the highest nonlinear coefficient of the material, allows walk-off-free phase matching and permits easy selection of any desired signal–idler wavelength pair within the material transparency that fulfils energy and momentum conservation relations, by engineerable design of the grating in the bulk material. Currently, QPM nonlinear crystals such as periodically poled $LiNbO_3$ (PPLN) and the arsenate isomorphs of $KTiOPO_4$, namely $KTiOAsO_4$ (PPKTA) and $RbTiOAsO_4$ (PPRTA), offer the most viable material candi-

dates for high-repetition-rate mid-infrared pulse generation. The large optical nonlinearity of these materials combined with a NCPM capability, an absorption edge below 500 nm and a transparency range extending to $> 5\,\mu$m allows the development of practical synchronously pumped OPOs for the mid-infrared using widely available near-infrared pump sources based on mode-locked neodymium or Kerr-lens-mode-locked (KLM) Ti:sapphire lasers. The potential of this approach has been previously demonstrated in a Ti:sapphire laser pumped picosecond OPO based on PPRTA, tunable in the 3.3–5-μm spectral range [9]. Using PPLN as the nonlinear crystal and a mode-locked diode-pumped Nd:YLF laser as the pump source, an all-solid-state picosecond OPO has also been demonstrated with a tunable range to 5.3 μm [10].

In this paper we describe picosecond pulse generation in the mid-infrared using a singly resonant OPO based on PPLN and synchronously pumped by a KLM Ti:sapphire laser. The important advantage of a Ti:sapphire laser is a pump tuning capability that allows rapid and flexible OPO tuning over extensive wavelength regions at a fixed crystal temperature, even using a single grating. We demonstrate operation of the OPO using both standard and semi-monolithic cavity configurations. Using the semi-monolithic cavity design we have obtained a minimal threshold of oscillation and extended idler tuning well into the strong absorption region of PPLN, and have extracted usable output power at idler wavelengths in the mid-infrared.

1 Experimental

1.1 Standard cavity design

Quasi-phase-matched tuning characteristics in periodically poled crystals show that wide wavelength tunability can be achieved either by changing the grating period of the crystal or by changing the pump wavelength. In materials that exhibit temperature-dependent refractive index, wavelength tuning can also be obtained by changing the crystal temperature at a fixed grating period and pump wavelength. In PPLN under Ti:sapphire pumping, all three mechanisms are available for wavelength tuning. In Fig. 1a and b the calculated tuning characteristics of PPLN under first-order quasi-phase matching are plotted as a function of Ti:sapphire pump wavelengths for different grating periods at temperatures of 130 °C and 180 °C, respectively. The calculations are based on the Sellmeier equations of [11]. It can be seen that idler tuning in the 4–6-μm spectral range can be readily achieved for Ti:sapphire pump wavelengths from 835 nm to 960 nm over a range of crystal temperatures using a grating period of 21.0–22.4 μm.

In our experiments, we used a PPLN crystal incorporating eight gratings, equally spaced in period from 21.0 to 22.4 μm. The crystal length was determined from considerations of group velocity walk-off between the pump and the resonant signal. In Fig. 2a and b the calculated temporal walk-off for PPLN in terms of the inverse group velocity mismatch between the pump, signal and idler is plotted across the potential mid-infrared tuning range of the OPO for crystal temperatures of 130 °C and 180 °C, respectively. The calculations are again based on temperature-dependent dispersion equations

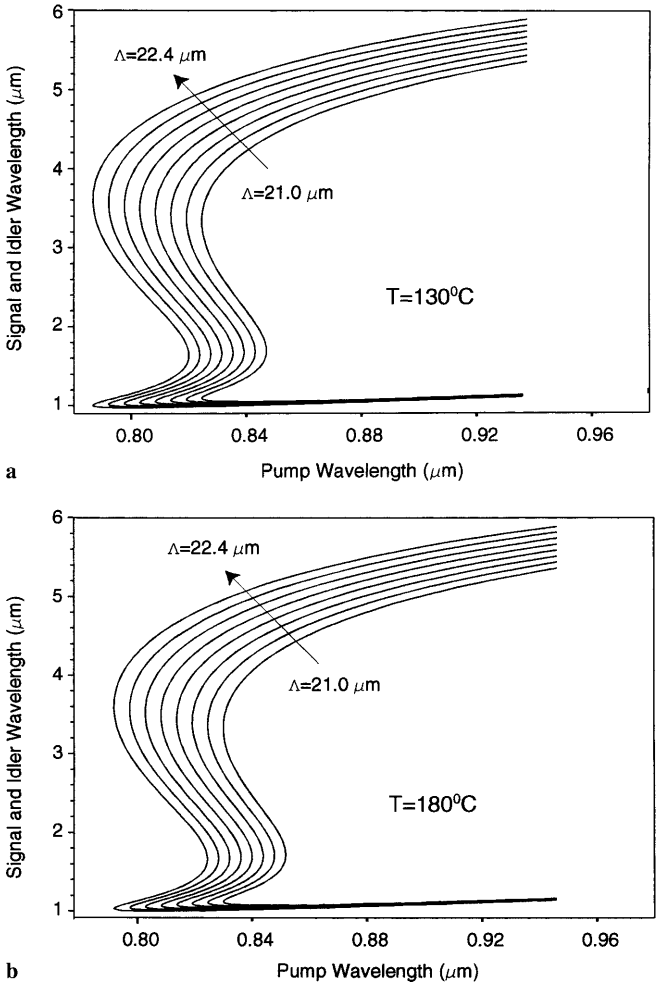

Fig. 1a,b. Pump tuning characteristics of PPLN optical parametric oscillator at **a** 130 °C and **b** 180 °C for grating periods from 21.0 to 22.4 μm, in steps of 0.2 μm. The calculations are based on the Sellmeier equations of [11]

for PPLN provided in [11]. It can be seen that the temporal walk-off between the pump and signal amounts to about 100 and 200 fs/mm, whereas the pump and idler walk-off is on the order of 200 to −700 fs/mm across the idler tuning range. The temporal walk-off between the signal and idler is in the range of 0 to −800 fs/mm across this tuning range. Since in the singly resonant oscillator, the walk-off between the pump and the resonant wave has a predominant effect on OPO performance, we chose a crystal length of 6 mm for the ∼ 1-ps pump pulses used in these experiments. The crystal had a $0.5 \times 11\,\text{mm}^2$ aperture and was cut for NCPM along the optical x-axis. To avoid photo-refractive damage, the crystal was maintained at $> 120\,^\circ$C in a servo-controlled oven and the crystal temperature could be varied to an accuracy of $\pm 0.1\,^\circ$C using a precision controller. The pump, signal and idler were all polarised along the optical z-axis for $e \rightarrow e + e$ interaction, hence accessing the largest nonlinear tensor element (d_{33}) in PPLN.

The experimental arrangement of the singly resonant OPO in standard cavity configuration is shown in Fig. 3. The cavity is a three-mirror folded arrangement, formed by two concave mirrors M_1 and M_2, each having radius of curvature $r = -150$ mm, and a plane mirror M_3. The mirror M_1 (CaF_2 substrate) was coated for high transmission

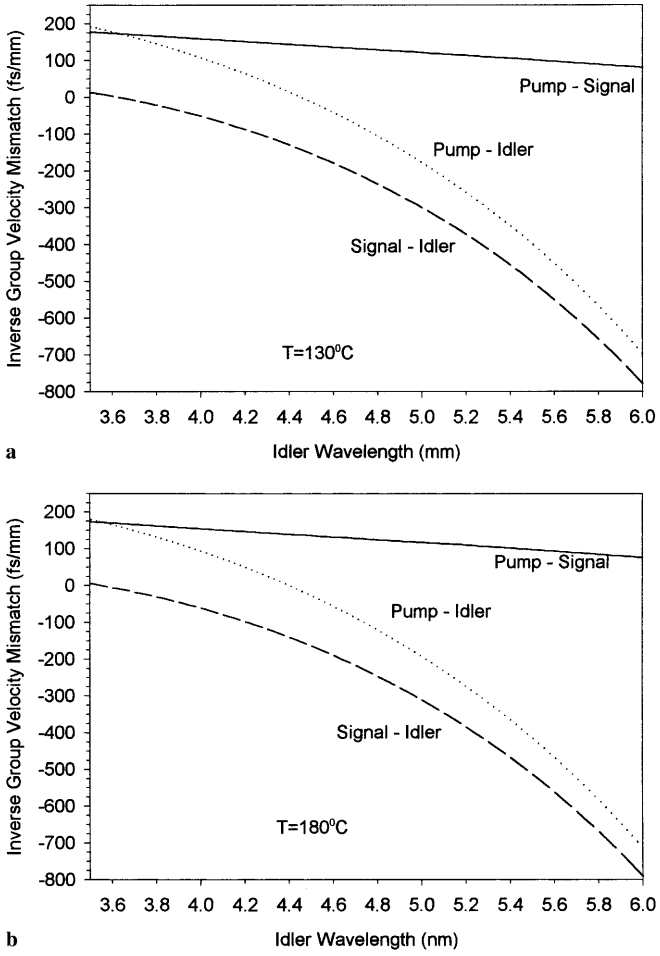

Fig. 2. Inverse group velocity mismatch in PPLN for mid-infrared parametric generation in the 3–6-μm spectral range pumped by a Ti:sapphire laser. The *solid line* represents the inverse group velocity mismatch ($1/v_{ps} = 1/v_p - 1/v_s$) between pump and signal pulses, while the dotted line is that between the pump and idler pulses ($1/v_{pi} = 1/v_p - 1/v_i$). The *dashed line* is the mismatch ($1/v_{si} = 1/v_s - 1/v_i$) between the signal and idler pulses

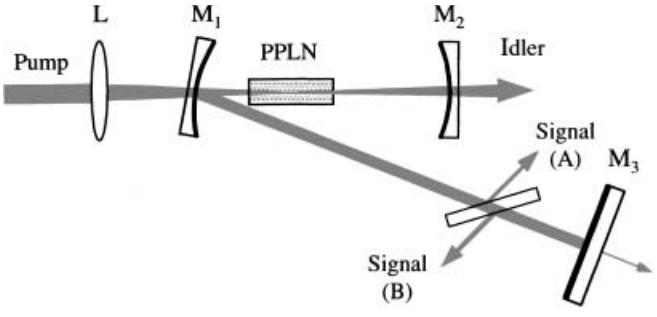

Fig. 3. Schematic of the experimental arrangement for the singly resonant PPLN optical parametric oscillator in standard cavity configuration. M_1 and M_2 are concave mirrors ($r = -150$ mm), while M_3 is a plane high-reflector. Signal output coupling is achieved using an intracavity Brewster plate

($T > 99\%$) at pump wavelengths (835–1000 nm) and had high reflectivity ($R > 99.5\%$) over the signal wavelength range (1.00–1.10 μm). The mirror M_2 (CaF_2 substrate) was also coated for high reflectivity ($R > 99.5\%$) at the signal wavelengths and high transmission ($T > 90\%$) at the idler wavelengths (3–6 μm). The cavity was completed with a plane mirror M_3 having high reflectivity ($R > 99.5\%$) at the signal wavelengths. The pump beam was focused to a waist radius of 20 μm at the centre of the crystal using a two-lens combination, each having a focal length of −70 mm and +100 mm. Both faces of the crystal were also anti-reflection-coated at the pump and signal wavelengths. The OPO was synchronously pumped by a KLM Ti:sapphire laser (Spectra-Physics, Tsunami), which was itself pumped by a 5-W frequency-doubled Nd:YVO_4 laser (Spectra Physics, Millennia). Configured with a long-wavelength mirror set, the laser delivered a power of 980 to 250 mW over the wavelength range of 0.835 to 1.0 μm, in pulses of ∼ 1.0-ps duration at 80.5-MHz repetition rate. A Faraday isolator was introduced between the OPO and the pump laser to avoid any feedback into the pump laser and a half-wave plate was used to control the polarisation state of the pump beam.

In this cavity configuration we achieved an idler tuning range from 4.1 to 5.5 μm with the available grating periods, by tuning the pump from 845 to 910 nm. The corresponding signal tuning range was from 1010 nm to 1100 nm. The signal wavelengths were recorded using a silicon detector and a spectrum analyser, and the corresponding idler wavelengths were directly measured by a liquid nitrogen cooled InSb detector through a monochromator. The mid-infrared idler tuning range was restricted to 5.5 μm due to the increase in the OPO power threshold, which could not be overcome with the available pump power. The rise in the OPO threshold is due mainly to the increase in PPLN absorption loss at longer idler wavelengths [12].

The output power at the idler as well as signal wavelengths was measured using a pyroelectric power meter. The residual pump and visible light generated in this system were cut out by a coated Ge filter before measurements of output power. As the output power was dependent on the OPO cavity length, the resonator length was adjusted to extract the maximum output power on changing the pump wavelength. It was observed that the OPO could be operated over a cavity detuning range of $\delta L \sim 70$ μm. Taking account of the transmission loss of the coated Ge filter, the maximum idler output power measured after the filter was 24 mW at 4.65 μm, decreasing to ∼ 1 mW at 5.5 μm. The measured mid-infrared idler power as a function of idler wavelength is shown in Fig. 4. It is clear that the idler power decreases with the increase in idler wavelength, mainly due to the rise in crystal absorption loss at longer wavelengths [12]. The decrease is also attributed in part to the reduction in the available pump power at longer wavelengths, from 980 mW at 835 nm to 250 mW at 960 nm.

Also shown in Fig. 4 is the measured threshold pump power for the OPO at different idler wavelengths. In this cavity configuration the lowest threshold pump power, measured at the input face of the crystal, was about ∼ 160 mW at 4.3 μm, increasing to ∼ 460 mW at 5.5 μm. It is seen from the plot that threshold pump power increases with increasing idler wavelengths, again as a result of the decrease in crystal transmission [12] at longer idler wavelengths. Comparison of the data of Fig. 4 with PPLN transmission characteristics [12] indicates that the idler power and the OPO pump power threshold closely follow the mid-infrared transmission characteristics of the material.

We also measured the output power in the resonant signal beam. In the absence of suitable output couplers, an uncoated glass slide was introduced into the OPO cavity near

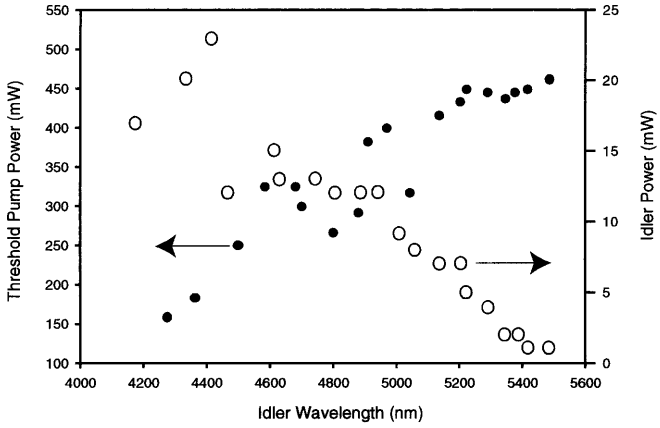

Fig. 4. Measured threshold pump power (*filled circles*) and the mid-infrared output power (*open circles*) across the idler tuning range of the standard-cavity PPLN OPO

Brewster's angle to allow extraction of signal power. By adjusting the angle of the glass plate about the Brewster condition, we were able to vary the output coupling loss from the OPO and thus maximise the extracted power in the signal beam. As can be seen from Fig. 3, the signal output could be extracted from the glass plate in two beams. In Fig. 5, the extracted signal power in each beam and the total power are plotted as a function of signal wavelengths. The maximum total power in the two beams was 95 mW, measured at a wavelength of 1048 nm.

The temporal characteristics of the signal pulses were also recorded by two-photon intensity autocorrelation measurements using an AlGaAs photodiode [13]. A representative autocorrelation recorded at a signal wavelength of 1038 nm is shown in Fig. 6a, with the corresponding spectrum depicted in Fig. 6b. The signal pulse width is 1.3 ps (assuming a sech^2 pulse shape) and the spectrum is 4.9 nm (full-width at half-maximum), resulting in a time–bandwidth product of 1.77. This implies that in the absence of dispersion compensation, the signal pulses are chirped and about 5 times the transform limit. The inclusion of intracavity dispersion compensation

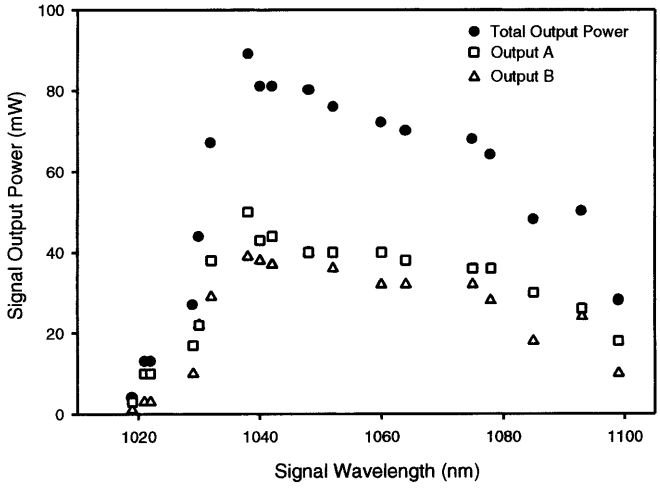

Fig. 5. Extracted signal power from the PPLN OPO in standard-cavity configuration using an uncoated Brewster plate. The different sets of data and the corresponding designations refer to the beam directions as shown in Fig. 3

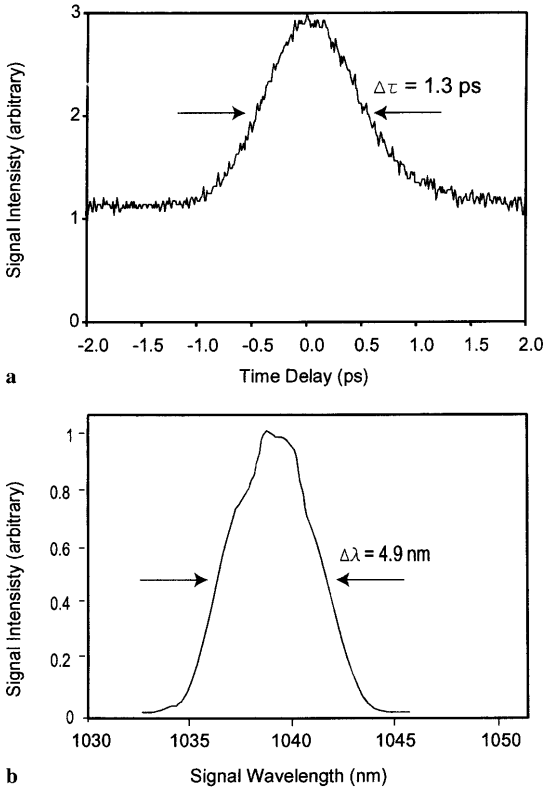

Fig. 6. a Temporal characteristics of the signal pulse at 1038 nm from standard-cavity OPO, recorded by intensity autocorrelation using an AlGaAs photodetector, showing a full-width at half maximum (FWHM) duration of 1.3 ps (assuming a sech^2 pulse shape). **b** The corresponding signal spectrum, exhibiting a FWHM bandwidth of 4.9 nm

should allow the generation of chirp-free signal pulses with a time–bandwidth product close to the transform limit. However, in this cavity configuration no attempt was made to implement dispersion compensation.

1.2 Semi-monolithic cavity design

In the standard cavity configuration, the maximum idler output power from the OPO was 24 mW, the longest idler wavelength was 5.5 μm and pump power thresholds of 160 to 460 mW were measured across the tuning range. The OPO performance was limited primarily by the rapid rise in the idler absorption loss of PPLN in the mid-infrared, making pulse generation at practical powers beyond 5 μm increasingly difficult. One technique to overcome this limitation has been to use a high-power mode-locked and amplified Nd:YLF laser to allow mid-infrared generation in a PPLN picosecond OPO in the strong idler absorption region to 6.3 μm [14]. A second technique has been based on the use of high-peak-power femtosecond pulses from an argon-ion-pumped KLM Ti:sapphire laser to achieve large parametric gain in a short crystal of PPLN, thus allowing tuning into the second transmission window of the material for the extraordinary polarisation to 6.8 μm [12]. In our experiments we used a different approach to the generation of mid-infrared radiation in the strong idler absorption region of PPLN based on a semi-monolithic cavity design for the OPO in combination with an all-solid-state pump source [15]. The approach is attractive

because it can be implemented with low- to moderate-power picosecond pump sources without the need for amplification and can also be extended to other continuous-wave or pulsed laser sources.

In the semi-monolithic cavity design used here, the pump and signal field are hemispherically focused onto the output facet of the nonlinear crystal [16, 17]. Since in the strong idler absorption limit, the generated mid-infrared power is determined by the mixing of signal and pump over the last extinction length of the crystal [14], hemispherical focusing allows the enhancement of idler power by maximising the pump and signal intensities over the final absorption length of the crystal. The semi-monolithic cavity configuration also results in low intracavity loss by minimising the number of cavity components and coated intracavity surfaces, leading to a low operation threshold and improved stability. It also avoids the need for specialist mid-infrared mirror substrates (e.g. CaF_2 or ZnSe) and provides a highly convenient experimental arrangement for the collection and collimation of the idler light, where absorption through optical coatings and mirror substrates, beam divergence and quantum defect generally limit maximal extraction and usability of the mid-infrared output.

The configuration of the semi-monolithic OPO is shown in Fig. 7. The singly resonant cavity is similar to that described in Sect. 1.1 (Fig. 3), with the modification that the output mirror through which the idler is extracted (M_2 in Fig. 3) is now coated directly onto the exit facet of the nonlinear crystal. The coated face provides $> 99\%$ reflectivity over the signal wavelength range (1.010–1.100 μm) and $> 90\%$ transmission over the idler range (3–6 μm). The input facet is anti-reflection-coated ($R < 0.25\%$) over 1.010–1.1 μm and has $> 98\%$ transmission for the pump at 835–1000 nm. The cavity is completed by an input concave mirror ($r = -150$ mm), through which the pump is focused to a waist radius of ~ 20 μm on the exit facet of the crystal (M_1) and a plane mirror (M_2). To offset any increase in threshold due to hemispherical focusing, the coated output facet of the crystal is also highly reflecting ($R > 99\%$) for the pump to allow double-pass pumping of the OPO. This is also enables convenient filtering of the pump light from the idler output at the exit facet of the crystal. The PPLN crystal used in this experiment was identical to that used in the standard cavity OPO in every respect, except for the reflective coating on the output facet as described above. All other experimental conditions were also similar to those used in the standard cavity experiments.

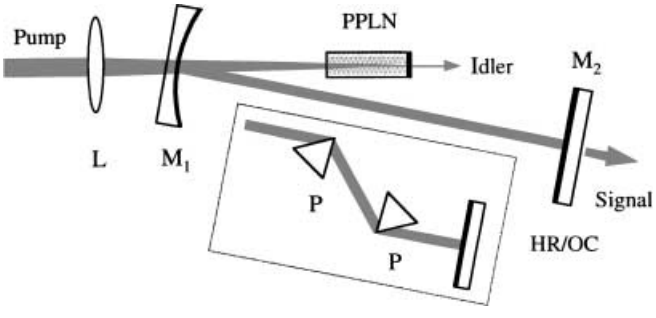

Fig. 7. Cavity configuration of the semi-monolithic singly resonant PPLN optical parametric oscillator. M_1 is a concave mirror ($r = -150$ mm) and M_2 is a plane reflector through which the signal beam is extracted. The idler beam is extracted directly through the output facet of the PPLN crystal. P refers to SF14 prisms

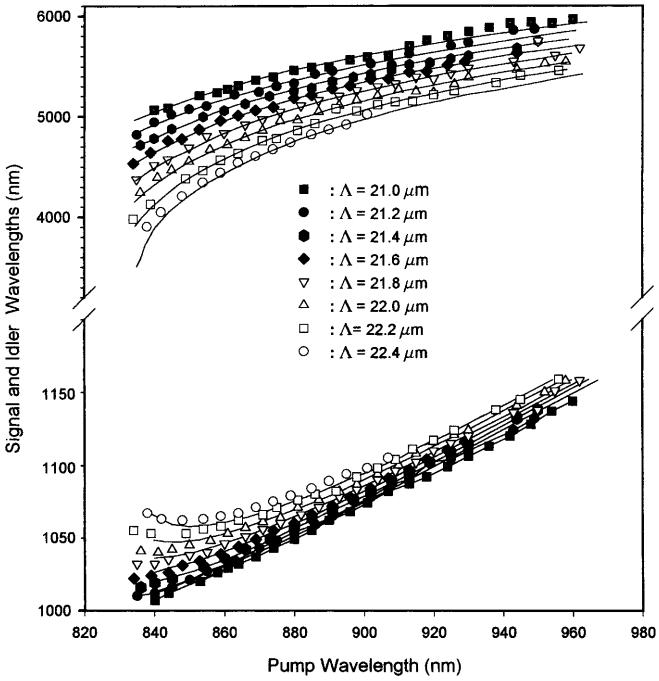

Fig. 8. Measured pump tuning range of the singly resonant semi-monolithic PPLN OPO for different grating periods at 180 °C. The *solid curves* are the theoretical calculations based on the Sellmeier equations of [11]

The tuning characteristics of the semi-monolithic OPO are shown in Fig. 8. In these experiments, the idler beam was conveniently collected using a single CaF_2 collimating lens after the PPLN crystal and a Ge filter was used to cut out any residual pump and generated visible light. The idler beam was then directly measured on a nitrogen-cooled InSb detector through a monochromator. The signal beam was also measured directly using a silicon detector and a spectrum analyser. The tuning data correspond to a fixed crystal temperature of 180 °C, and the solid curves represent the theoretical tuning range obtained from the Sellmeier equations of [11]. With the available gratings, the OPO was tuned from 3.9 to 5.98 μm in the idler, corresponding to 1.004 to 1.140 μm in the signal over a pump tuning range of 835–960 nm. The longest idler wavelength of 5.98 μm was obtained for a grating period of 21.0 μm at a pump wavelength of 960 nm. Wavelength tuning was also readily available at other crystal temperatures, or at a fixed pump wavelength and crystal temperature through grating tuning. This multi-parameter tuning capability can be of utility in pump–probe measurements requiring a specific combination of more than two spectral components simultaneously.

The mid-infrared tuning coverage and the longest idler wavelength of 5.98 μm obtained here represent significant improvements over the standard cavity OPO under the same operating conditions. In this case, the limit to the mid-infrared tuning range was set by the available grating periods, whereas for the standard cavity this limit was due to the large increase in the OPO threshold in the mid-infrared, which could not be overcome with the available pump power. Also shown in Fig. 9 are representative idler spectra directly recorded from the OPO. The spectral bandwidth of the idler is typic-

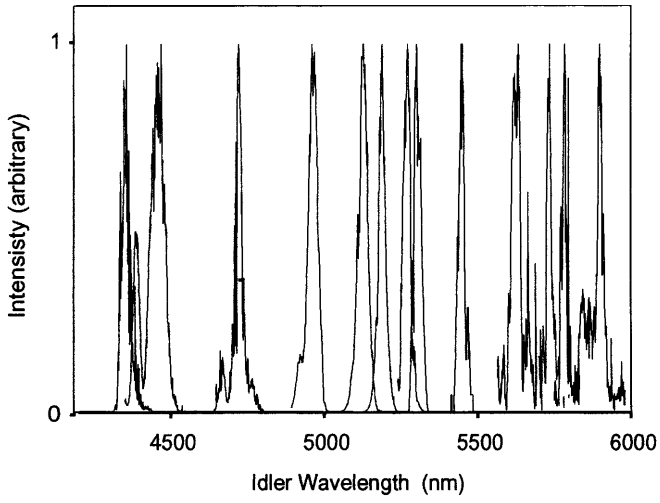

Fig. 9. Normalised mid-infrared idler spectra from the semi-monolithic PPLN OPO. The longest recorded idler wavelength is centred at 5.89 μm

ally ~ 26 nm (FWHM), with the longest spectrum extending to 6 μm. We were also able to operate the semi-monolithic OPO with increased signal output coupling by replacing the high reflector mirror, M_2 in Fig. 7, with two mirrors having reflectivities of 93% and 80% at a centre wavelength of 1.064 μm. This resulted in a reduction in the overall tuning range of the OPO, with the longest idler wavelength reduced to 5.87 μm and 5.69 μm for the 7% and 20% output couplers, respectively.

The mid-infrared idler power characteristics of the semi-monolithic OPO were also investigated for different levels of signal output coupling and the results are plotted in Fig. 10. The data correspond to the one-way idler power exiting the output facet of the PPLN crystal and represent directly measured values on a pyroelectric power meter, after correction for ~ 10% idler loss through the uncoated CaF_2 lens and the coated Ge filter. The highest recorded idler power was 64 mW at 4.3 μm, which was obtained with no signal output coupling. Under this condition, idler output powers of > 45–60 mW were measured over the 4.1–5.2-μm spectral range, with > 45 mW available to 5.2 μm. We were able to measure idler powers of > 10 mW to 5.5 μm and > 0.5 mW out to 5.9 μm. Because of double-pass pumping, similar amounts of idler power are also generated in the opposite direction and exit the OPO cavity through the input mirror (M_1 in Fig. 7). The mid-infrared idler powers obtained here are significantly higher than those generated with the standard cavity OPO under the same operating conditions, hence demonstrating the advantages of the semi-monolithic approach. It can also be seen from Fig. 10 that the increase in signal output coupling from the OPO resulted in a decrease in the extracted idler power as expected.

Measurements of idler output power as a fraction of the input pump power across the idler tuning range are plotted in Fig. 11. The data were obtained under the conditions of minimum signal output coupling. The maximum one-way conversion efficiency from the input pump to the idler output power was ~ 9% at 4.9 μm, with a corresponding slope efficiency of ~ 12%. Higher idler powers and efficiencies were hampered by the large transmission loss of uncoated optical components between the Ti:sapphire laser and the PPLN crystal, which resulted in a 20%–35% reduction in the available pump power across the pump tuning range. We also note that, in addition to the increasing crystal absorption loss and quantum defect, the decline in the idler power at wavelengths beyond 5.5 μm is strongly correlated with the decrease in the Ti:sapphire pump power at longer wavelengths as discussed earlier. With the use of a 10-W primary Nd:YVO4 laser, a longer-wavelength mirror set for the Ti:sapphire laser, improvements in pump transmission optics and additional PPLN grating periods, we expect a substantial increase in the idler power from the semi-monolithic OPO at wavelengths out to 7 μm.

The average pump power threshold for the semi-monolithic OPO across the idler tuning range is shown in Fig. 12 for different signal output couplers. The data correspond to the pump power at the input to the nonlinear crystal. As evident from the plot, with minimum signal output coupling, the power threshold remains below 100 mW for wavelengths up to ~ 5.5 μm, with the lowest threshold of 17 mW recorded at ~ 4.3 μm. Beyond 5.5 μm, the threshold steadily rises due to the increasing absorption loss, measuring ~ 275 mW at

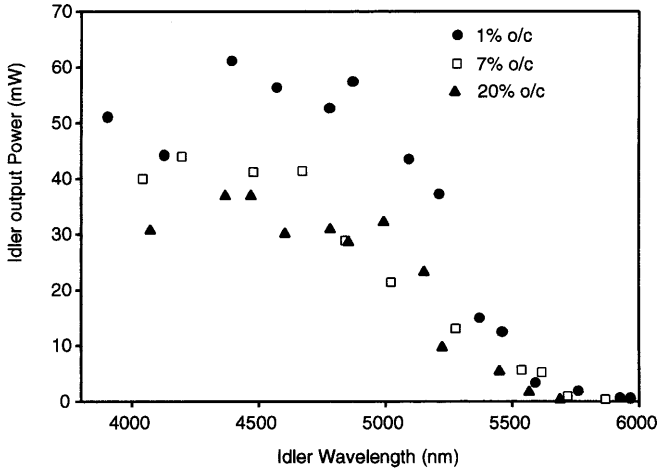

Fig. 10. Extracted idler power across the mid-infrared tuning range of the semi-monolithic OPO for three different levels of signal output coupling between ~ 1% and ~ 20%

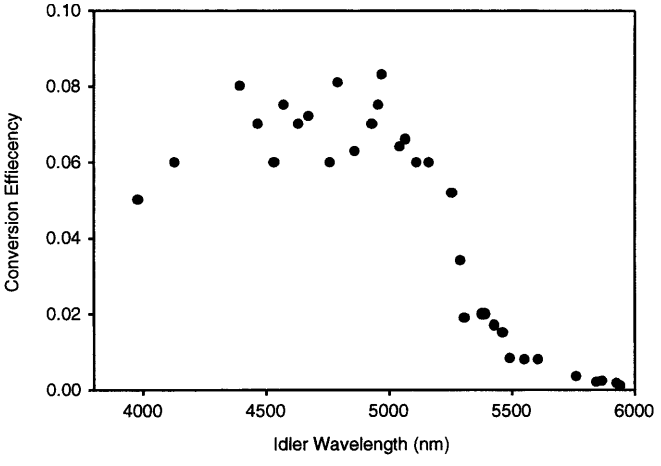

Fig. 11. Measured conversion efficiency from the input pump power to the output idler power across the mid-infrared tuning range of the semi-monolithic PPLN OPO. The data were obtained under conditions of minimal signal output coupling

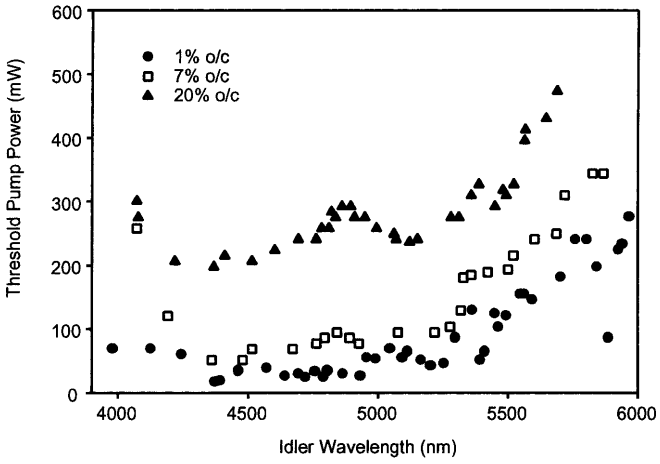

Fig. 12. Threshold pump power of the semi-monolithic OPO in the mid-infrared as a function of the idler wavelength for three different levels of signal output coupling between ~ 1% and ~ 20%

~ 6 μm. The minimum threshold of 17 mW obtained here is almost an order of magnitude lower than the corresponding value of 160 mW recorded at the same wavelength in the standard cavity OPO. Moreover, the semi-monolithic OPO threshold remains below the minimum standard cavity threshold of 160 mW over much of the mid-infrared tuning range out to ~ 5.5 μm, even with the ~ 7% signal output coupling. The observed threshold behaviour of the semi-monolithic OPO is also in close agreement with the PPLN crystal transmission loss across the demonstrated tuning range [12]. The measured mid-infrared power thresholds are also, to our knowledge, the lowest values in the strong idler absorption region of PPLN beyond 5 μm, hence demonstrating the advantage of the semi-monolithic cavity design.

In addition to mid-infrared idler power, we were able to extract useful signal output in the near-infrared with the available output couplers. In Fig. 13, the extracted signal powers for different output mirrors with transmissions of < 1%, ~ 7% and ~ 20% are plotted across the signal tuning range. We obtained a maximum signal power of 280 mW at 1.038 μm for 800 mW of pump power with the ~ 20% output coupler, representing a signal extraction efficiency of ~ 35%. With the available input pump power usable signal powers in excess of 150 mW could be extracted over the 1.004–1.080-μm spectral range with both output couplers. The output signal power as a function of pump power for the different output couplers was also investigated. The maximum signal slope efficiency was ~ 46%, obtained with the ~ 20% output coupler at 1.038 μm. As expected, the increase in signal output coupling resulted in a reduction in idler power and a corresponding increase in OPO threshold (see Figs. 10 and 12). With the ~ 20% output coupler, we observed a near three-fold increase in threshold and reduction in idler output of between 20% and 50% across the OPO tuning range. However, we were still able to simultaneously extract 0.2–40 mW of idler together with 50–250 mW of signal over > 80% of the tuning coverage out to 5.7 μm.

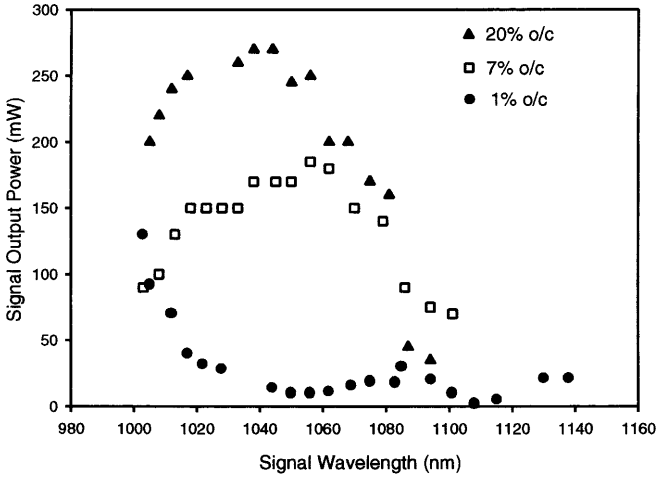

Fig. 13. Extracted signal power from the semi-monolithic PPLN OPO as a function of signal wavelength for three different levels of signal output coupling between ~ 1% and ~ 20%

Without dispersion compensation and in the absence of signal output coupling, oscillation of the semi-monolithic OPO could be maintained over a cavity mismatch range of $\delta L \sim 250$ μm. At optimum cavity synchronous length, the signal spectra were characterised by strong self-phase modulation (SPM) over a bandwidth of ~ 50 nm. An interesting phenomenon that we observed with the semi-monolithic OPO was the simultaneous oscillation of several output frequen-

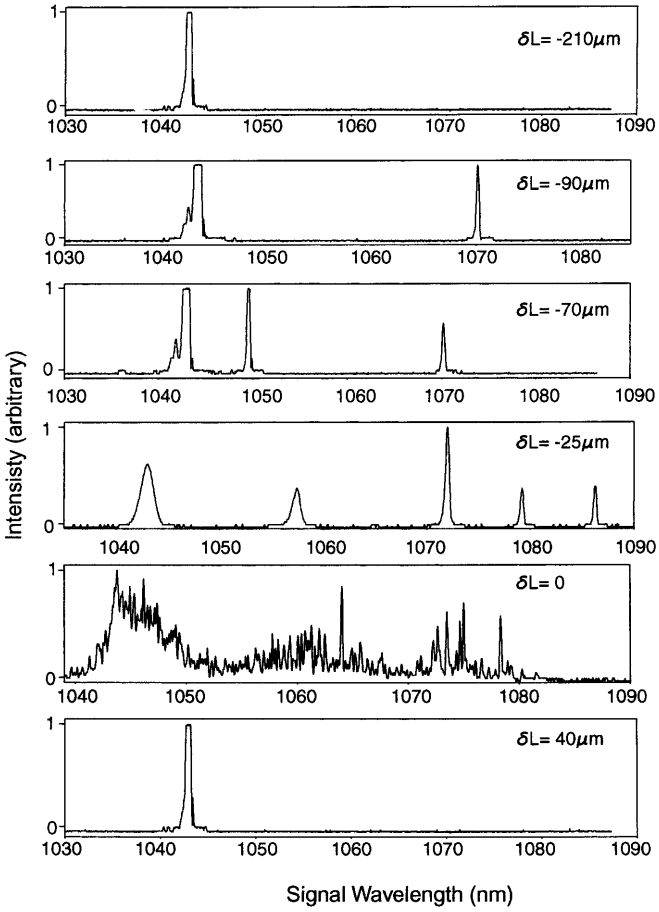

Fig. 14. Spectral behaviour of the signal pulses from the semi-monolithic PPLN OPO with the change in the cavity synchronous length. The spectra were recorded in the absence of intracavity dispersion compensation and with minimum signal output coupling. The optimum cavity synchronous length ($\delta L = 0$) corresponds to the position of maximum signal power and self-phase-modulated spectrum

cies on changing the cavity length. With tuning the cavity length, we consistently observed modification of the SPM signal spectrum and the appearance of up to 5 distinct spectral components over the ~ 50-nm spectral range, separated by ~ 10 nm, decreasing in number with the reduction in the synchronous length, as shown in Fig. 14. The corresponding idler also exhibited similar behaviour. With minimum signal output coupling, the multi-chromatic emission was observed over almost the entire OPO tuning range. However, on increasing the signal output coupling to 7% and 20%, we observed a reduction in the number of discrete spectral components with the accompanying decrease in cavity length mismatch range and a reduction in intracavity SPM. Similar multi-chromatic emission has been observed in a femtosecond OPO based on PPLN [18] and the exact cause of the multi-chromatic emission is currently under investigation.

With the ~ 20% output coupler, we observed smooth signal spectra with a bandwidth of ~ 7 nm (FWHM), the absence of SPM or the distinct spectral components and a reduction in the cavity mismatch range to $\delta L \sim 100\,\mu$m at full pump power. Temporal characterisation of the signal pulses was performed using a two-photon autocorrelator based on a AlGaAs light-emitting diode [13]. Without dispersion compensation, the signal pulses had a duration of 0.44 ps (a sech^2 pulse shape being assumed), with a time–bandwidth product of ~ 0.37. A typical autocorrelation and spectrum of the signal pulse at a wavelength of 1.023 μm is shown in Fig. 15. The signal pulse characteristics were also found to remain uniform across the tuning range. In an effort to obtain chirp-free pulses, we implemented intracavity dispersion compensation using a pair of Brewster-angled SF14 prisms (see Fig. 7). This resulted in the generation of transform-limited signal pulses with durations of 0.4 ps and a time–bandwidth product of 0.34. The insertion loss introduced by inclusion of the intracavity prism pair resulted in a reduction in the idler tuning range to 5.79 μm and a cavity synchronous range to $\delta L = 170\,\mu$m with minimal signal output coupling.

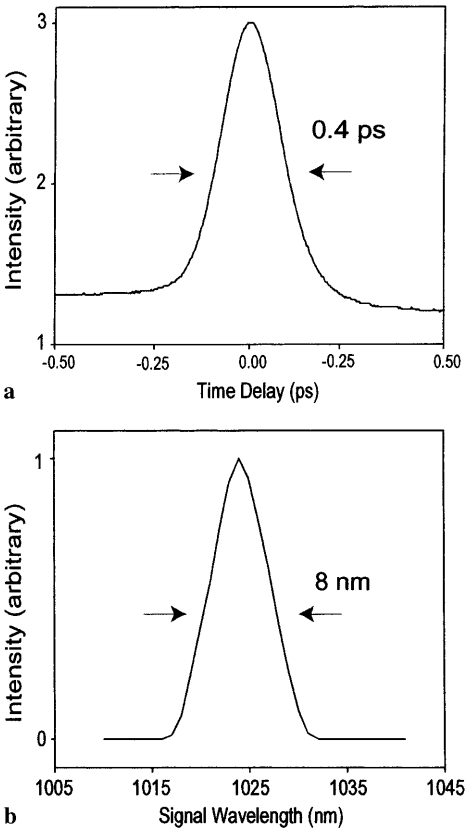

Fig. 15. a Intensity autocorrelation of the signal pulses from the semi-monolithic PPLN OPO at a wavelength of 1023 nm with ~ 20% output coupling. The FWHM pulse duration is 0.4 ps (assuming a sech^2 pulse shape). **b** The corresponding signal spectrum, exhibiting a FWHM bandwidth of 8 nm

The low intracavity loss of the semi-monolithic OPO allowed the generation of signal pulses at harmonics of the fundamental frequency of 80.5 MHz through reduction in the OPO synchronous length. Oscillation was readily achieved

Table 1. Comparison of performance of a semi-monolithic and a standard cavity PPLN OPO

	Semi-monolithic cavity						Standard cavity
	Without dispersion compensation					With dispersion compensation	
Signal output coupling		< 1%		< 7%	< 20%	< 1%	< 1%
OPO repetition rate (MHz)	322	161	80.5	80.5	80.5	80.5	80.5
Threshold pump power (mW)	233.5	122	17	53.5	87	60	160
Maximum idler power (mW)	30	40	64	44	38	50	24
Idler tuning range (μm)	3.9 – 5.6	3.9 – 5.94	3.9 – 5.98	4.04 – 5.87	4.07 – 5.69	3.9 – 5.79	4.1 – 5.5
Maximum signal power (mW)	110	120	130	180	280	50	90
Signal tuning range (μm)	1.004– 1.080	1.004– 1.121	1.004– 1.144	1.022– 1.133	1.022– 1.124	1.004– 1.127	1.010– 1.100
Cavity mismatch range (μm)	20	40	250	200	100	170	70
Cavity length (cm)	~ 46.4	~ 92.8	~ 185.6	~ 185.6	~ 185.6	~ 185.6	~ 185.6

at 161 MHz and 322 MHz by simply translating the signal output mirror (M_2 in Fig. 7) to yield a two-fold or four-fold reduction in the cavity length, respectively. This resulted in a highly compact OPO cavity, which at 322 MHz measures only ~ 46 cm in total length. Because of the consequent increase in the round-trip signal loss, OPO operation at 161 and 322 MHz was characterised by an increase in threshold and a small reduction in the overall tuning range. Although in either case no attempt was made to re-optimise mode matching, we were still able to extract significant amounts of signal and idler power from the OPO and extended mid-infrared tuning. The performance characteristics of the semi-monolithic OPO under different operating conditions are summarised in Table 1.

2 Conclusions

In conclusion, we have described the generation of tunable high-repetition-rate pulses in the mid-infrared using optical parametric oscillation in PPLN, synchronously pumped by a Kerr-lens-mode-locked Ti:sapphire laser. We have achieved low pump power thresholds, useful output powers and efficiencies and extended tuning beyond 5 μm in the mid-infrared in an all-solid-state configuration. The significant advantages of the semi-monolithic design and hemispherical focusing over the standard cavity configuration for wavelength generation in the strong idler absorption region of the material have been demonstrated. This approach has resulted in the development of a compact, efficient and robust source of mid-infrared pulses with a pump power threshold as low as 17 mW, idler power of as much as 64 mW and wavelength coverage to 6 μm at 80.5 MHz. We have also demonstrated reliable operation of the OPO at harmonics of the fundamental repetition frequency of 161 and 322 MHz. These characteristics make the device a versatile and convenient source of ultra-short mid-infrared pulses for spectroscopic applications.

Acknowledgements. This work was supported by the EPSRC under Grant No. GR/L61637. The authors are also grateful to the Royal Society and the Commonwealth Scholarship Commission for partial support of this research.

References

1. G.C. Bhar, S. Das, U. Chatterjee, P.K. Datta, Y.N. Andreev: Appl. Phys. Lett. **63**, 1316 (1993)
2. E. Takaoka, K. Kato: Opt. Lett. **24**, 903 (1999)
3. Y.N. Andreev, I.S. Baturin, P.P. Geiko, A.I. Gusamov: Quantum Electron. **29**, 904 (1999)
4. K. Kato, E. Takaoka, N. Umemura, T. Chonan: Conf. Lasers and Electro-Optics, San Francisco, USA (2000) paper CTuA9
5. W. Kein, S. Hahn: J. Appl. Phys. **58**, 4594 (1985)
6. J.C. Mikkelson, H. Kildal: J. Appl. Phys. **49**, 426 (1978)
7. V.V. Badikov, I.N. Matveev, V.B. Panyutin, S.M. Pshenichnikov, A.E. Rozenson, S.V. Skrebena, N.K. Trotsenko, N.D. Ustinov: Sov. J. Quantum Electron. **10**, 1302 (1980)
8. L.E. Myers, R.C. Eckardt, M.M. Fejer, R.L. Byer, W.R. Bosenberg, J.W. Pierce: J. Opt. Soc. Am. B **12**, 2102 (1995)
9. G.T. Kennedy, D.T. Reid, A. Miller, M. Ebrahimzadeh, H. Karlsson, G. Arvidsson, F. Laurell: Opt. Lett. **23**, 503 (1998)
10. L. Lefort, K. Puech, S.D. Butterworth, G.W. Ross, P.G.R. Smith, D.C. Hanna, D.H. Jundt: Opt. Commun. **152**, 55 (1998)
11. D.H. Jundt: Opt. Lett. **22**, 1553 (1997)
12. P. Loza-Alvarez, C.T.A. Brown, D.T. Reid, W. Sibbett, M. Missey: Opt. Lett. **24**, 1523 (1999)
13. D.T. Reid, M.J. Padgett, C. McGowan, W.E. Sleat, W. Sibbett: Opt. Lett. **22**, 233 (1999)
14. L. Lefort, K. Puech, G.W. Ross, Y.P. Svirko, D.C. Hanna: Appl. Phys. Lett. **73**, 1610 (1998)
15. P.J. Phillips, S. Das, M. Ebrahimzadeh: Appl. Phys. Lett. **77**, 469 (2000)
16. E.O. Ammann, P.C. Montgomery: J. Appl. Phys. **41**, 5270 (1970)
17. G.D. Boyd, F.R. Nash: J. Appl. Phys. **42**, 2815 (1971)
18. K.C. Burr, C.L. Tang, M.A. Arbore, M.M. Fejer: Appl. Phys. Lett. **70**, 3341 (1997)